International Journal of Heat and Mass Transfer 54 (2011) 1598–1607

Contents lists available at ScienceDirect

International Journal of Heat and Mass Transfer

journal homepage: www.elsevier.com/locate/ijhmt

Transitional flow inside enhanced tubes for fully developed and developing flow with different types of inlet disturbances: Part II–heat transfer

J.P. Meyer *, J.A. Olivier

Department of Mechanical and Aeronautical Engineering, University of Pretoria, Pretoria, South Africa

ARTICLE INFO

Article history:
Received 26 March 2010
Accepted 21 November 2010
Available online 24 December 2010

Keywords:
Heat transfer
Diabatic
Friction factor
Pressure drop
Enhanced tubes
Transition
Fully developed flow
Developing flow
Single-phase
Inlet
Disturbance

ABSTRACT

Due to efficiency demands, augmented tubes are often used in heat exchangers with the result that many heat exchangers operate in the transitional region of flow. Due to the paucity of data, however, no data exists for enhanced tubes in this region. This article, being the second of a two-part paper (Part I investigating adiabatic flow), presents experimental heat transfer and diabatic friction factor data for four horizontal enhanced tubes for fully developed and developing flow in the transition region with four different types of inlet geometries. Smooth tube data was used for comparison. It was found that, unlike results obtained for adiabatic flow in Part I, inlet disturbances had no effect on the critical Reynolds numbers, with transition occurring at a Reynolds number of approximately 2000 and ending at 3000. Correlations were developed to predict the heat transfer and friction factors for a wide range of flow regimes, from laminar to turbulent flow. The correlations predicted the heat transfer data on average with a mean absolute error of 9.5%, predicting 85% of the data to within 15%. The friction factor correlations predicted the data with a mean absolute error of 5.5%, predicting 96% of the data to within 20%.

© 2010 Elsevier Ltd. All rights reserved.

1. Introduction

Transition from laminar to turbulent flow inside smooth tubes occurs at a Reynolds number of 2300. However, transition in reality occurs in a wide range of Reynolds numbers, varying between 2300 and 10,000 [1]. In this range, flow instabilities occur and large pressure variations are encountered as the pressure gradient required to accelerate the flow from laminar to turbulent flow could vary by an order of magnitude. Therefore, it is normally advised when designing heat exchangers to remain outside the transitional range due to uncertainty of this region. However, due to environmental concerns, enhanced tubes are employed to design more efficient heat exchangers, such as chiller units, decreasing the required mass flow rate for a given heat transfer rate, causing the heat exchangers to operate in or near the transitional flow regime.

Transition was shown by Reynolds [2] to depend on surrounding disturbances and the Reynolds number. Just above the critical value, turbulence would occur in flashes or turbulent bursts at a fixed point down the length of the tube, which was also visually observed by Lindgren [3]. Lindgren found that the transition occurred in a gradual manner with fluctuating bursts of turbulence. The frequencies of these bursts were found to be a function of the fluid velocity and the distance from the inlet. It was also shown that the critical Reynolds number increased with an increase in distance from onset, with visual observations confirming this. Kalinin and Yarkho [4] found with heat transfer experiments that the wall temperatures start to fluctuate in the transition region. Ede [5] also detected the fluctuations although they were blamed on a technical issue.

Inlet profiles were found to have a profound influence on the transition Reynolds number. Nagendra [6] found that the greater the disturbance, the earlier transition occurs. Ghajar and Madon [7] performed an extensive study into the effect of three different types of inlets on the critical Reynolds number during isothermal fully developed flow. The three inlets tested were a square-edged (sudden contraction), a re-entrant (tube-protruding square-edged inlet) and a bellmouth inlet (smooth, gradual contraction). It was found that transition from laminar to turbulent flow occurred at Reynolds numbers of 1980–2600 for the re-entrant, 2070–2840 for the square-edged and 2125–3200 for the bellmouth inlet. A study performed by Smith [8] indicated that transition occurred in the inlet length of the tube and not in the fully developed Poiseuille region. This, combined with the work of Ghajar and Madon, shows that the inlet acts as a disturbance to the flow, which they also concluded. Results published in later work by Tam and Ghajar [1] showed transition to occur at different

* Corresponding author.
E-mail address: josua.meyer@up.ac.za (J.P. Meyer).

0017-9310/$ - see front matter © 2010 Elsevier Ltd. All rights reserved.
doi:10.1016/j.ijheatmasstransfer.2010.11.026

Nomenclature

A	Area (m^2)
A_c	Actual tube flow cross-sectional area (m^2)
A_{cn}	Nominal cross-sectional area based on root diameter (m^2)
A_{core}	Core flow area $(A_n(1-2e/D_r)^2)$ (m^2)
A_{fin}	Inner-fin flow area $(A_c - A_{core})$ (m^2)
A_i	Inner-tube heat transfer surface area (m^2)
A_n	Nominal heat transfer surface area based on root diameter (m^2)
A_o	Annulus heat transfer surface area (m^2)
$c_{1...9}$	Constants
D	Diameter (m)
D_i	Tube inner-wall diameter (m)
D_o	Tube outer-wall diameter (m)
D_r	Root diameter (m)
e	Fin, dimple or roughness height (m)
h_{iin}	Inner-tube inlet enthalpy (J/kg)
h_{iout}	Inner-tube outlet enthalpy (J/kg)
h_{oin}	Annulus inlet enthalpy (J/kg)
h_{oout}	Annulus outlet enthalpy (J/kg)
j	Colburn j-factor
k_{cu}	Thermal conductivity of copper tube (W/mK)
L	Tube length (m)
$L_{\Delta p}$	Pressure drop length (m)
L_{hx}	Heat transfer length (m)
l_c	Characteristic length (m)
l_{csw}	Characteristic length modified for swirling flow (m)
$\dot{m}_i$	Mass flow rate within inner tube (kg/s)
$\dot{m}_o$	Mass flow rate within annulus (kg/s)
N	Number of fins
p	Pressure (Pa)
p_f	Fin pitch (m)
$\dot{Q}_i$	Inner-tube heat transfer rate (W)
$\dot{Q}_o$	Annulus heat transfer rate (W)
R_w	Wall thermal resistance (K/W)
s	Average fin thickness (m)
$\overline{T}_{Cu}$	Mean temperature of copper tube (K)
T_i	Mean inner-tube fluid temperature (°C)
$\overline{T}_{iin}$	Inner-tube inlet temperature (°C)
$\overline{T}_{iout}$	Inner-tube outlet temperature (°C)
T_{lmtd}	Logarithmic mean temperature difference (°C)
T_o	Annulus fluid bulk temperature (°C)
$\overline{T}_{oin}$	Annulus inlet temperature (°C)
$\overline{T}_{oout}$	Annulus outlet temperature (°C)
$\overline{T}_{wi}$	Mean inner-tube inner-wall temperature (°C)
$\overline{T}_{wo}$	Mean inner-tube outer-wall temperature (°C)
U	Overall heat transfer coefficient (W/m^2K)
u	Average fluid velocity (m/s)

Dimensionless groups

eb	Energy balance
f	Darcy friction factor
f_e	Enhanced tube Darcy friction factor
f_{Le}	Enhanced tube laminar Darcy friction factor
f_s	Smooth tube Darcy friction factor
f_{te}	Enhanced tube transition Darcy friction factor
Gr	Grashof number
Nu	Nusselt number
Nu_e	Enhanced tube Nusselt number
Nu_{Le}	Enhanced tube laminar Nusselt number
Nu_s	Smooth tube Nusselt number
Nu_{te}	Enhanced tube transition Nusselt number
$Nu_{Te_{38}}$	Enhanced tube Nusselt number for $3000 \leqslant Re \leqslant 8000$
Pr	Prandtl number
Ra	Rayleigh number
Re	Reynolds number of inner tube
Re_{cr}	Critical Reynolds number

Greek symbols

α_i	Inner-tube heat transfer coefficient (W/m^2K)
α_o	Annulus heat transfer coefficient (W/m^2K)
β	Helix angle (°)
γ	Fin apex angle (°)
μ	Inner-fluid bulk viscosity (Pa.s)
μ_w	Inner-fluid viscosity at tube wall (Pa.s)
ρ	Density (kg/m^3)
σ_f	Friction factor standard deviation
σ_j	Heat transfer coefficient standard deviation

Subscripts

exp	Experimental
pred	Predicted

Reynolds numbers (much higher) than previous results. The transition for the re-entrant inlet started and ended at 2900–3500, for the square-edged at 3100–3700 and for the bellmouth at 5100–6100. Once again, though, it is clear that the inlet disturbance influences the critical point where transition occurs.

Heat transfer results by Ghajar and Tam [9] also showed that transition varied from inlet to outlet. For the re-entrant inlet, it started and ended at a Reynolds number of 2000 and 6700, respectively, near the inlet of the tube (three diameters from the inlet) and 2100 and 8500 near the exit (192 diameters from the inlet). For the square-edged inlet, these limits were 2400–7300 and 2500–8800 while for the bellmouth, they were 3400–9400 and 3800–10,500. Ghajar and Tam [10] explained this variation from inlet to outlet to the variation in fluid properties. Since the tube was under a uniform heat flux boundary, the fluid was heated along the axial length with the effect of the viscosity decreasing and hence an increase in Reynolds number. Correlations were developed to predict the critical Reynolds numbers for the different inlets. Further correlations were also developed to predict heat transfer in the transition region of flow.

Mori et al. [11] performed tests using air with two types of inlets; one with a disturbance at the inlet, which generated turbulence, and the other without. The tests with the disturbance revealed that as the Rayleigh number (accounting for buoyancy-induced secondary flows) was increased, the critical Reynolds number increased. The reason for this is that the secondary flow suppresses the turbulence being created by the disturbance. For tests with no disturbance, it was found that the critical Reynolds number decreased with an increase in Rayleigh number due to the secondary flow actually generating the turbulence. They observed that when $ReRa$ was large, the secondary flow caused the critical Reynolds numbers to tend to the same value, whether the turbulence level at the entrance of the tube was high or low. Heat transfer also had an effect on the laminar friction factor, increasing with the amount of heat being added [1]. This effect was also observed by Nunner [12] while performing heat transfer experiments. The increase (as much as 100%) was attributed to the buoyancy-induced secondary flows altering the velocity profile, which, in turn, influences the shear stress at the tube wall.

Transition is also affected by the type of tube augmentation. Nunner [12] found that transition was accelerated by the severity of the augmentation. Nunner inserted different types of circular rings at different distances along the length of the tube. For the same diameter tubes, laminar heat transfer results of the

augmented tubes were not significantly higher than those of the smooth tube. Obot et al. [13] analysed the results of previous research performed on transition flow. Specifically by reanalysing the results of Nunner [12] and Koch [14], it was found that the main contributing factor concerning transition was the roughness height.

Extensive augmentation work in the turbulent regime has been performed between Reynolds numbers of 2000 and 150,000 mostly with water, although some data is on air and glycol–water mixtures. Most of the research was performed by heating the fluid, although there were some researchers who performed the experiments on the cooling of the liquid. The augmentation techniques used were internally finned tubes [15], some with single-helix ridging [16], others with multi-helix ridging [17], micro-finned tubes [18–20], V-nozzle turbulators [21] and finned inserts [22].

For augmentation in the laminar flow regime, most of the experiments were conducted with twisted tape inserts [23–26] with only a few on micro-finned tubes [25]. Reynolds numbers ranged between 15 and 30,000 with water and oil being the main fluids. These experiments were also mostly conducted on the heating of the fluid with only a few performing heating and cooling experiments.

In the transition regime, the experiments were performed on the heating of the fluid, except for those conducted by Manglik and Bergles [24], who also investigated flow in the transition region by means of the cooling of the fluid. Most of the augmentation techniques involved the inserts of tapes [24] and wire coils [27,28]. No helical finned-type tubes have yet been tested in this region. The fluids used were a mixture of water and ethylene/propylene glycol.

The aim of this paper is to present heat transfer and friction factor results for water for helical finned tubes in the transition region for fully developed and developing flow with different types of inlets. The data is to be compared with existing laminar and turbulent correlations for smooth and enhanced tubes and a new correlation in the transition region for enhanced tubes will be presented. This paper is the second of a two-part paper and focusses on heat transfer, while the first paper [29] focusses on adiabatic pressure drops.

2. Data reduction

The details of the experimental facility were discussed in detail in Part I by Meyer and Olivier [29] and will not be repeated here. The inner tube's average heat transfer coefficient was obtained by making use of the overall heat transfer coefficient and the sum of the resistances, given by

$$\alpha_i = \frac{1}{A_i}\left[\frac{1}{UA} - R_w - \frac{1}{\alpha_o A_o}\right]^{-1} \tag{1}$$

UA can be obtained by making use of the heat transfer as well as the log-mean temperature difference, as

$$UA = \frac{\dot{Q}_i}{T_{lmtd}} \tag{2}$$

where $\dot{Q}_i$ is given by

$$\dot{Q}_i = \dot{m}_i(h_{iin} - h_{iout}) \tag{3}$$

and similarly the heat transfer in the annulus by

$$\dot{Q}_o = \dot{m}_o(h_{oout} - h_{oin}) \tag{4}$$

with the enthalpies obtained from the IAPWS [30], which is directly related to the local specific heat and temperature values.

The heat transfer in the inner tube was compared with that in the annulus by means of an energy balance, given by

$$eb = \frac{\dot{Q}_i - \dot{Q}_o}{\dot{Q}_i} \times 100 \tag{5}$$

Although good energy balances were obtained, the inner-tube heat transfer rate was used for all the calculations as it was the more accurate of the two. This was because the annulus flow rate was kept high such that its thermal resistance was as low as possible. The consequence was that the temperature difference between the inlet and outlet of the annulus was much smaller than that of the inner tube, giving the heat transfer rate of the annulus a larger uncertainty than that of the inner tube. The resistance of the annulus was approximately 6% of that of the inner tube.

The log-mean temperature difference used in Eq. (2) is given by

$$T_{lmtd} = \frac{(\overline{T}_{iin} - \overline{T}_{oout}) - (\overline{T}_{iout} - \overline{T}_{oin})}{\ln\left(\frac{\overline{T}_{iin} - \overline{T}_{oout}}{\overline{T}_{iout} - \overline{T}_{oin}}\right)} \tag{6}$$

The wall resistance in Eq. (1) is obtained by

$$R_w = \frac{\ln(D_o/D_i)}{2\pi k_{cu} L_{hx}} \tag{7}$$

The thermal conductivity of the copper was obtained from [31] and is given by

$$k_{cu} = a\overline{T}_{Cu}^{b} e^{c\overline{T}_{Cu} + d/\overline{T}_{Cu}} \tag{8}$$

where the constants $a = 82.56648$, $b = 0.262301$, $c = -4.06701 \times 10^{-4}$ and $d = 59.72934$. $\overline{T}_{Cu}$ is the mean temperature of the copper tube in Kelvins.

As a first approximation, the wall temperature on the outer surface of the inner tube was used for T_{Cu} to calculate the tube's thermal conductivity. After this, the temperature of the inner-wall of the inner tube was calculated. The average of the outer-wall and the inner-wall temperature was then used to calculate a new thermal conductivity value, with the process being repeated until the solution converged. The influence of the wall resistance on the heat transfer coefficient in all cases, however, was found to be negligible.

Lastly, the annulus heat transfer coefficient was calculated by making use of the annulus outer-wall temperature and the temperature of the outer-wall of the inner tube, all of which were measured. Thus,

$$\alpha_o = \frac{\dot{Q}_i}{A_o(\overline{T}_{wo} - \overline{T}_o)} \tag{9}$$

Since the wall temperatures were measured along the length of the heat exchanger, an appropriate average value was used for all calculations. This average value was obtained by integrating the temperature as a function of the axial length position and dividing by the total length of the heat exchanger. The *trapezoidal rule* instead of a curve fit was used due to it resulting in a lower uncertainty.

The Darcy–Weisbach friction factor was determined from the pressure drop, Δp, as

$$f = \frac{2D\Delta p}{\rho u^2 L_{\Delta p}} \tag{10}$$

The inside diameter was used for the smooth tubes while the envelope diameter was used for the enhanced tubes. The average velocity was determined from the measured mass flow rate and the cross-sectional flow area. For the enhanced tubes, the actual cross-sectional area was determined by the method explained by Lambrechts [32]. The fluid properties were calculated at the average inner-tube fluid temperature, which was determined by the resulting heat transfer coefficient, Eq. (1), as

$$\overline{T}_i = \frac{\dot{Q}_i}{\alpha_i A_i} + \overline{T}_{wi} \tag{11}$$

This temperature was also used to determine the Reynolds, Prandtl, Nusselt and other dimensionless groups with the fluid properties being obtained from Wagner and Pruß [33].

Heat transfer results are presented in terms of the Colburn j-factor, defined as

$$j = \frac{Nu}{RePr^{1/3}} \tag{12}$$

Table 1 lists the experimental parameters and their accompanying uncertainties. These uncertainties not only include those due to propagation of error, but also the random errors obtained from the experimental measurements. It can be seen that the uncertainties of the heat transfer coefficients and Nusselt numbers are very low; less than 2%.

3. Validation

Friction factors were validated in the papers of Olivier and Meyer [34] and Part I of this paper (Meyer and Olivier [29]), and will therefore not be repeated here. Heat transfer validation for laminar and turbulent fully developed flow was performed inside a smooth tube (R_1). Fig. 1 shows the experimental heat transfer data in terms of j-factors for a Reynolds number range of 1000–12,000. The data consisted of a total of 2097 data sets with 100 data points per set (logged at a frequency of 1.5 Hz, giving a total of 209,700 points). The data sets consisted of both increasing and decreasing increments of the Reynolds number. Also shown on the graph are the Sieder and Tate [35] correlation for turbulent flow and the correlations of Oliver [36] and Shome and Jensen [37] for laminar flow. The laminar flow correlations incorporate the effects of buoyancy-induced secondary flows (mixed convection), which improve the heat transfer, as shown on the graph when compared with the line ($j = 3.662/RePr^{1/3}$) for fully developed laminar flow for a constant wall temperature boundary and no buoyancy effects. It was shown in Olivier and Meyer [34] that the laminar heat transfer is in the mixed convection flow regime as defined by the Metais and Eckert [38] flow pattern map.

The Sieder and Tate [35] correlation predicts the turbulent heat transfer data ($Re \geqslant 3000$) with a mean absolute error of 2%, predicting 96% of the data to within 10%. The laminar correlations of Oliver [36] and Shome and Jensen [37] (lying very close to each other) predict the data with a mean absolute error of 1.7% and 1%, respectively, predicting 90% and 94% of the data to within 10%, respectively. From these results, it can be concluded that the experimental system is validated.

Table 1
Experimental range and uncertainties.

	Value	Uncertainty
$\dot{m}_i$ (kg/s)	0.006–0.265	0.1–4.3%
$\overline{T}_{iin}/\overline{T}_{iout}/\overline{T}_{oin}/\overline{T}_{oout}$ (°C)	20.35–65.67	0.011–0.46
$\overline{T}_o$ (°C)	20.9–23.67	0.014–0.032
$\overline{T}_{wo}$ (°C)	21.33–25.53	0.011–0.055
$\overline{T}_{wi}$ (°C)	21.34–25.61	0.011–0.055
$\overline{T}_i$ (°C)	32.98–41.97	0.176–0.857
T_{lmtd} (°C)	12.16–18.18	0.172–0.855
$\dot{Q}_i$ (W)	1 598–10 954	0.71–0.49%
UA (W/K)	131.5–605.8	1.02–1.08%
Re	436–21,084	1–4.4%
Nu	13.06–62.20	1.44–1.58%
Pr	4.17–5.06	±1.42%
Δp (Pa)	13.5–7073	0.1–27.9%
α_i (W/m^{2}K)	558–2 710	1.04–1.22%
f	0.0172–0.192	0.58–55.7%

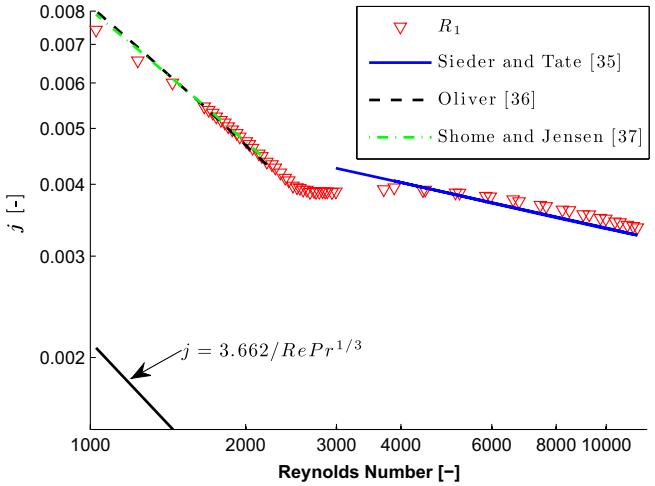

Fig. 1. Heat transfer results for a smooth tube for hydrodynamic fully developed flow. (For interpretation of the references to colour in this figure legend, the reader is referred to the web version of this article.)

4. Results

4.1. Heat transfer

The heat transfer coefficients for the enhanced tubes were calculated in terms of the nominal surface area, which is based on the nominal or root diameter. This approach is suggested by Marner et al. [39] and facilitates in the direct comparison of enhanced and smooth tube performance. Fig. 2 shows the fully developed and developing heat transfer results as j-factors for the smooth tubes as well as for the four enhanced tubes. Fig. 2a represents the smooth and enhanced tubes with a nominal diameter of 15.8 mm, while Fig. 2b represents those having a nominal diameter of 19.1 mm. The smooth tube data (spline through the data points in Fig. 1) is shown as a red line to aid in the comparison.

Turbulent results show that there is a definite increase in heat transfer with the use of the enhanced tubes, with the 27° tube showing the highest enhancement. It is further noted that the 19.1 mm enhanced tubes (Fig. 2b) have slightly higher values compared with the equivalent 15.8 mm tubes (Fig. 2a). This is due to the Prandtl numbers of the 19.1 mm tube being slightly higher than their 15.8 mm counterparts. Inlet disturbances have no effect on the turbulent regime.

Between Reynolds numbers of 3000 and 8000, the j-factors are actually increasing with Reynolds number, unlike the smooth tube results, which vary little. The increase is due to the fins breaking up the laminar viscous sublayer, which can account for up to 60% of a liquid's temperature drop during turbulent flow [40]. Since the fin-height-to-diameter ratios for all the enhanced tubes are almost the same, the further increase noticed would then be due to the helix angle, which, in turn, spins the fluid. This is seen for Reynolds numbers greater than 2600 and 2500 for the 15.8 mm and 19.1 mm enhanced tubes, respectively, where the 27° tubes start to deviate from the 18° tubes as the Reynolds number increases. This deviation would be due to the fins with the greater helix angle spinning the fluid more effectively, and hence aiding in the mixing thereof. Only after a Reynolds number of approximately 9000 do the enhanced tubes reach a maximum and stop to deviate from the smooth tube trend. The j-factors then start to decrease with increasing Reynolds number, following a parallel path with the smooth tube.

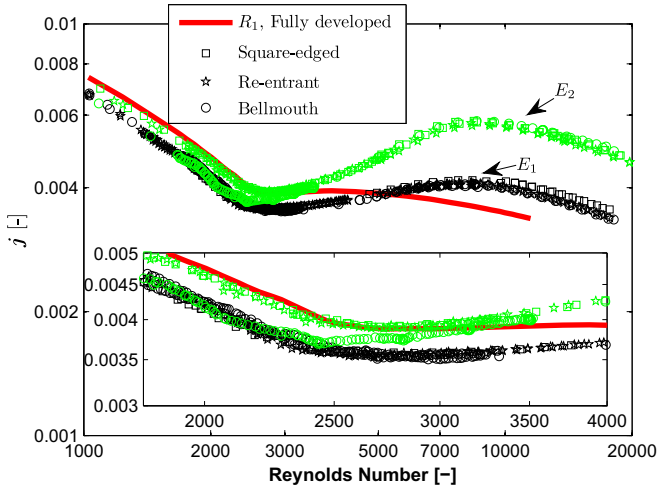

(a) Enhanced tubes E_1 and E_2

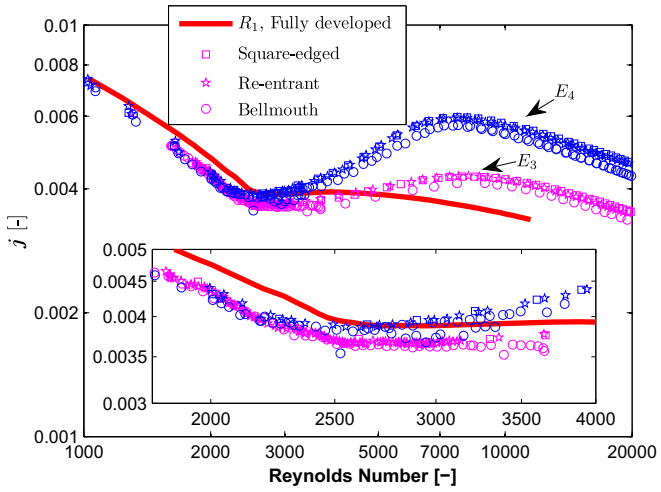

(b) Enhanced tubes E_3 and E_4

Fig. 2. Heat transfer results for smooth and enhanced tubes for developing and fully developed flow. The region for $Re = 1800 - 4000$ is enlarged and given as an insert. The red line is a spline fit of the smooth tube data given in Fig. 1.

For the laminar regime, it appears as if the enhanced tube heat transfer results are slightly lower than that of the smooth tubes. Furthermore, on closer inspection, it also appears that heat transfer for the 15.8 mm enhanced tubes are lower than that of the 19.1 mm tubes. The helix angle, however, has no noticeable effect on the laminar regime.

Thus, it seems that the fins have a negative influence on heat transfer in the laminar regime, although heat transfer values are still higher than the theoretical values for uniform wall heat flux ($Nu = 4.364$) and constant wall temperature ($Nu = 3.662$) boundaries. Since the enhancement of the laminar region is due to mixed convection, as observed by Olivier and Meyer [34], the fins could act as a restriction to secondary flows. Similar effects were observed by Vicente et al. [41] with the helical dimpled tubes at relatively low Rayleigh numbers ($10^4 - 10^6$). The Rayleigh numbers for the current experimental results were in the order of 10^6. This is shown in Fig. 3, which is a plot of the flow regime map of Metais and Eckert [38] with the fully developed enhanced tube and smooth tube data (the developing flow results are similar, but excluded for clarity). This figure shows that the potential for mixed convection for the enhanced tubes is roughly the same as for the smooth tubes. Thus, the only explanation for the lower

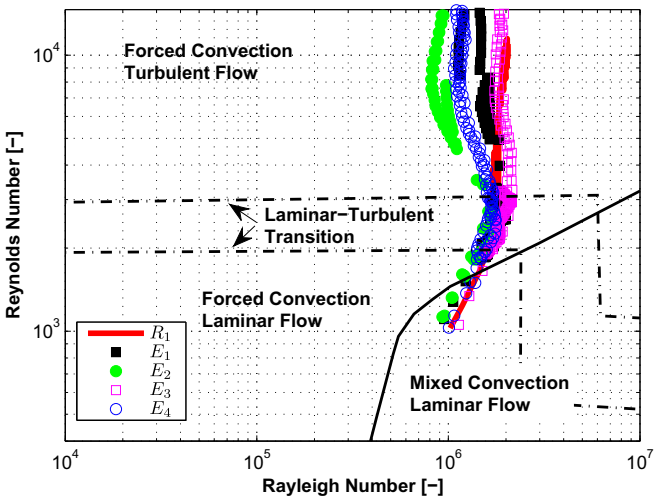

Fig. 3. Flow regime map of Metais and Eckert [38] for the smooth and enhanced tubes.

performance is that the fins partially obstruct the flow path for secondary flows. Note, though, that the mixed convection potential for heat transfer enhancement of the 19.1 mm tubes is greater than for the 15.8 mm tubes. This is reflected in the laminar heat transfer results.

What is further noted from this graph is the lower values of Ra for the enhanced tubes in the turbulent region. This shows that the fins aid in the mixing of the fluid, and subsequently the breaking of the laminar viscous sublayer. This is especially true after transition, as the mixed convection potential decreases for Reynolds numbers greater than the transition Reynolds numbers.

Transition for all the tubes and flow types, fully developed and developing flow, all appear to occur at roughly the same Reynolds numbers. This is in stark contrast to what was found for adiabatic flow, where transition was dependent on the tube type and inlet disturbance [29,34]. To verify this, the relative fluctuations of the Colburn j-factors as a function of Reynolds numbers are determined, which are given in Fig. 4. The relative fluctuations are determined by taking the ratio of the standard deviation of 100 measurements per data point and the average value of the same 100 measurements. To let all the data of the different tubes and

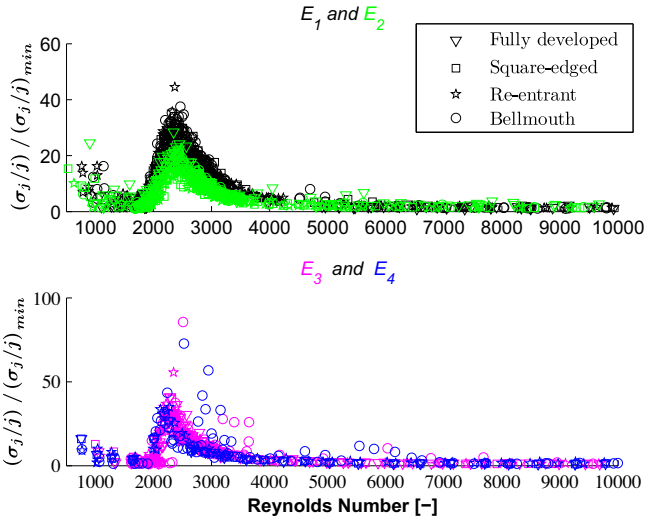

Fig. 4. Heat transfer relative fluctuations for smooth and enhanced tubes including various inlet disturbances.

inlets collapse, this ratio was divided by the minimum value of the ratio obtained for all the points. It is of interest to note that the fluctuations all occur at the same Reynolds numbers, starting at a Reynolds number of approximately 2000 and ending at 3000. This could be due to the secondary flows, which influence the growing boundary layer to such an extent that it negates any disturbance of the inlet. It also appears that roughness during heat transfer has little or no effect on the transition region. The only noticeable difference is in the percentage of fluctuation, although this difference is between the two diameter tubes and not between the smooth and enhanced tubes. The only discrepancies are for the bellmouth inlets for the 19.1 mm tubes (E_3 and E_4), which show a slight delay in transition. This, however, is also reflected in the heat transfer data of Fig. 2b.

4.2. Friction factor

The diabatic friction factors for the enhanced tubes are given in Fig. 5. Fig. 5a represents the data for tubes having a nominal diameter of 15.8 mm, while the data for tubes having a nominal diameter of 19.1 mm is given in Fig. 5b. For reference purposes, the laminar Poiseuille relation in terms of the Darcy friction factor as well as the Blasius correlation for turbulent flow is plotted as black solid lines. These results show that there is an overall increase in friction factor for the enhanced tubes compared with the smooth tubes, as was the case for the adiabatic results [29]. The turbulent results are very similar to those of the adiabatic friction factors, also having the same secondary transition region between a Reynolds number of 3000 and 10,000. These trends are also similar to the heat transfer results.

Enhanced tube diabatic friction factors in the laminar regime show that there is an increase in friction factors when compared with their adiabatic counterparts. These results are in line with the smooth tube results [34], with this increase being attributed to the secondary flow effects. The diabatic friction factors for the enhanced tubes, though, appear to be even higher than those found for the smooth tubes. Since the cause for the increase in friction factor for the smooth tubes was due to the secondary flow, it can be concluded that for the enhanced tubes the fins add to the extra increase.

However, there appears to be a difference between the different helix angles, with the 27° tubes showing the greatest increase. A reason for this increase could be related to the secondary flows and the fins. From the heat transfer results it was shown that the fins act negatively towards the heat transfer process in the laminar regime. It could be further argued that the fins act as a barrier for secondary flow, preventing the bulk of the fluid to mix with fluid at the tube wall. This could have the effect that the relatively unmixed liquid between the fins are at a cooler temperature than the rest of the fluid, thus having a higher viscosity and hence greater shear stress.

Transition for the enhanced tubes is also in the same region as that of their smooth tube counterparts, being between Reynolds numbers of 2000 and 3000. It appears that in this region the friction factors are independent of the Reynolds numbers. The critical Reynolds numbers, as was the case for the heat transfer results, are independent of the tube or type of inlet disturbance. What should be noted is that the friction factor results support the heat transfer results. This is important since the same results are obtained from totally independent measuring techniques. Fig. 6 shows the fluctuations of the friction factors as a function of the Reynolds number. This figure also confirms the friction factor results in terms of transition occurring between a Reynolds number of 2000 and 3000, unlike the adiabatic results where transition for the enhanced tubes occurred at a lower Reynolds number of approximately 1800.

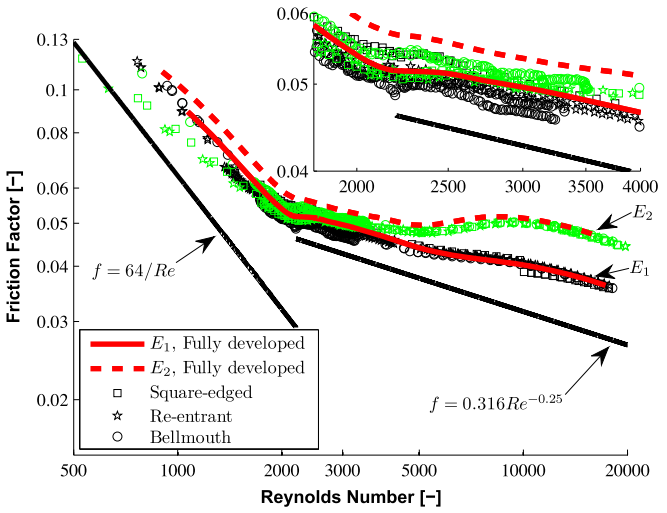

(a) Enhanced tubes E_1 and E_2

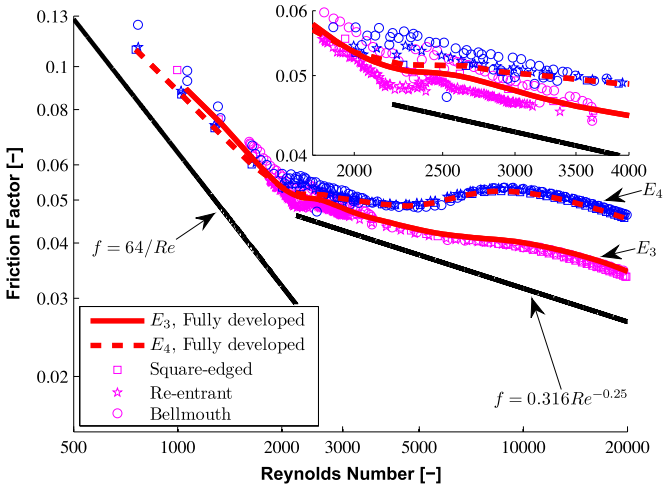

(b) Enhanced tubes E_3 and E_4

Fig. 5. Diabatic friction factor results for developing and fully developed flow for the 15.8 mm and 19.1 mm enhanced tubes. The Darcy friction factor for laminar fully developed flow ($f = 64/Re$) in a smooth tube and the Blasius equation for turbulent flow ($f = 0.316Re^{-0.25}$) in a smooth tube are plotted as solid black lines.

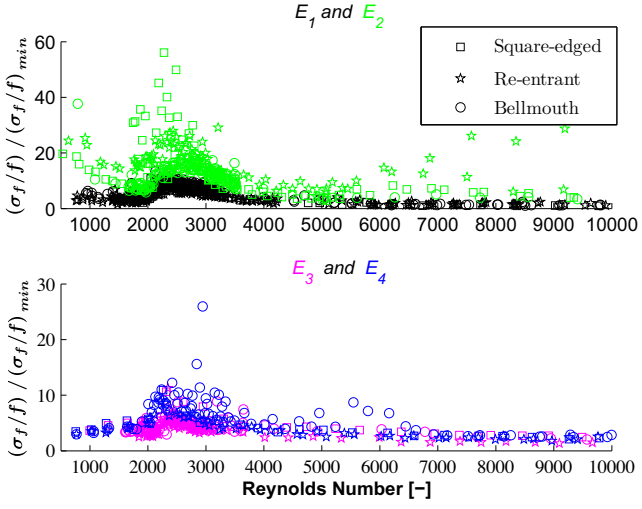

Fig. 6. Friction factor relative fluctuations for the enhanced tubes with different inlet disturbances.

5. Correlations

5.1. Comparison

Three turbulent heat transfer correlations relating to enhanced tubes are compared and are listed in Table 2. Fig. 7 shows the performance of these correlations against the experimental heat transfer data from a Reynolds number of 3000–20,000 (even though some of the correlations might not have been developed for this range).

The figure shows that the data deviates from all the correlations at a Reynolds number below approximately 8000. Above a Reynolds number of 8000, the Carnavos [15] correlation predicts the 18° tubes (E_1 and E_3) with good accuracy, while underpredicting the 27° tubes (E_2 and E_4). The Ravigururajan and Bergles [42] correlation overpredicts all the data although it seems to predict the 18° and 27° tubes with the same accuracy. The Jensen and Vlakancic [43] correlation appears to follow the right trend at low Reynolds numbers although it has the greatest scatter between different helix angles.

The Carnavos [15] correlation predicts all the data with a mean absolute error of 19%, predicting 62% of the data to within 15%. The Ravigururajan and Bergles [42] correlation predicts the data with a mean absolute error of 32%, predicting 26% of the data to within 15%, while the correlation of Jensen and Vlakancic [43] predicts the data with a mean absolute error of 16%, predicting 48% of the data to within 15%.

This is a pessimistic review of the results, since all the data deviates from the correlations at a Reynolds number below 8000. By only considering data above a Reynolds number of 8000, the correlation of Carnavos [15] predicts 100% of the data to within 15%, having a mean absolute error of 5.4%. The corresponding values for the Ravigururajan and Bergles [42] correlation are 57% of the data to within 15% and a mean absolute error of 15%, while those of the Jensen and Vlakancic [43] correlation are 68% of the data to within 15% with a mean absolute error of 12%.

Table 2
Heat transfer correlations for enhanced tubes.

Carnavos [15]

$$Nu_e = 0.023Re^{0.8}Pr^{0.4}(A_c/A_{cn})^{0.1}(A_n/A_i)^{0.5}(\sec\beta)^3 \quad (21)$$

$0 < \beta < 30^\circ,\ 10,000 < Re < 100,000,\ 0.7 < Pr < 30$

Ravigururajan and Bergles [42]

$$Nu_e = Nu_s\{1 + [2.64Re^{0.036}(e/D)^{0.212}(p_f/D)^{-0.21}(\beta/90)^{0.29}Pr^{0.024}]^7\}^{1/7} \quad (22)$$

$0.01 < e/D < 0.2,\ 0.1 < p_f/D < 7.0$

$0.3 < \beta/90 < 1.0,\ 5000 < Re < 250,000$

$0.66 < Pr < 37.6$

Jensen and Vlakancic [43]

$$Nu_e = Nu_s(l_c/D)^{-0.5}(A_{cn}/A_c)^{0.8}F \quad (23)$$

$$F = (A_i/A_n)^{0.29}[1 - 1.792(N\sin(\beta/\pi))^{0.64}(2e/D)^{2.76}Re^{0.27}]$$

$$l_c/D = A_{core}/A_c(1 - 2e/D) + A_{fin}/A_c[\pi/N(1 - 2e/D) - s/D]$$

$s = 4/3e\tan(\gamma/2) =$ average width of triangular fin

$2000 < Re < 80,000,\ Pr \approx 7$

$0 < \beta < 45^\circ,\ 0.0075 < e/D < 0.05$

5.2. Development of correlations

5.2.1. Laminar flow: heat transfer

From the results reported, it was postulated that the degradation in laminar heat transfer was due to the fins preventing/obstructing much of the secondary flow, which normally aids in the better mixing of the fluid. Since only the fin height would obstruct the secondary flow (no difference in results for different helix angles), the correlation developed for laminar flow inside smooth tubes [44] could be used to predict the enhanced tube data by including the fin-height-to-diameter ratio in the mixed convection term.

$$Nu_{Le} = 2.686\left[Re^{0.105}Pr^{1.133}\left(\frac{D}{L}\right)^{0.483} + 1.082\left(Gr^{0.362}Pr^{-2.987} \times \left(\frac{L}{D}\right)^{0.202}\left(\frac{e}{D}\right)^{0.0612}\right)^{0.277}\right]^{2.226}\left(\frac{\mu}{\mu_w}\right)^{0.152} \quad (13)$$

This correlation is valid for $1030 < Re < 2198,\ 4.58 < Pr < 5.67,\ 1.4 \times 10^5 < Gr < 2.5 \times 10^5,\ 0.7 < \mu/\mu_w < 0.847,\ 0.023 < e/D < 0.027$ and $286 < L/D < 349$.

5.2.2. Turbulent flow: heat transfer

It was seen from the previous section that the correlations of Carnavos [15] and Ravigururajan and Bergles [42] predicted the data with fair accuracy at Reynolds numbers greater than 8000. It will thus be attempted to develop a correlation for Reynolds numbers 3500–8000, which should then be used in conjunction with the mentioned correlations to predict heat transfer throughout the whole turbulent range.

Some of the parameters that will have an influence on this region will be the helix angle, fin pitch and roughness height. Thus, the correlation would be a function of fluid properties and tube geometrical properties,

$$Nu_{Te_{3\beta}} = f(Re, Pr, e, D, p_f, \beta) \quad (14)$$

It is proposed that the correlation have the form

$$Nu_{Te_{3\beta}} = c_1Re^{c_2}Pr^{c_3}\left(\frac{e}{D}\right)^{c_4}\left(\frac{p_f}{D}\right)^{c_5}\left(\frac{\beta}{90}\right)^{c_6} \quad (15)$$

By using a least-squares optimisation method, the constants were determined to be $c_1 = 0.35$, $c_2 = 1.33$, $c_3 = 1.19$, $c_4 = -0.11$, $c_5 = 2$ and $c_6 = 4.4$. This correlation is valid for $3500 \leqslant Re \leqslant 8000,\ 4.5 \leqslant Pr \leqslant 5.4,\ 18^\circ \leqslant \beta \leqslant 27^\circ,\ 0.176 \leqslant p_f/D \leqslant 0.387$ and $0.023 \leqslant e/D \leqslant 0.027$.

It should be noted that the relative roughness for the current tubes varied very little and that the value of its constant should be seen as tentative.

5.2.3. Transition flow: heat transfer

Since it was shown that transition follows a smooth path between laminar and turbulent flow with increasing Reynolds numbers, it would be best to combine the newly developed laminar and turbulent correlations to form a new transition correlation. This is done by following the approach of Churchill and Usagi [45]. The transition Reynolds number will then have the form

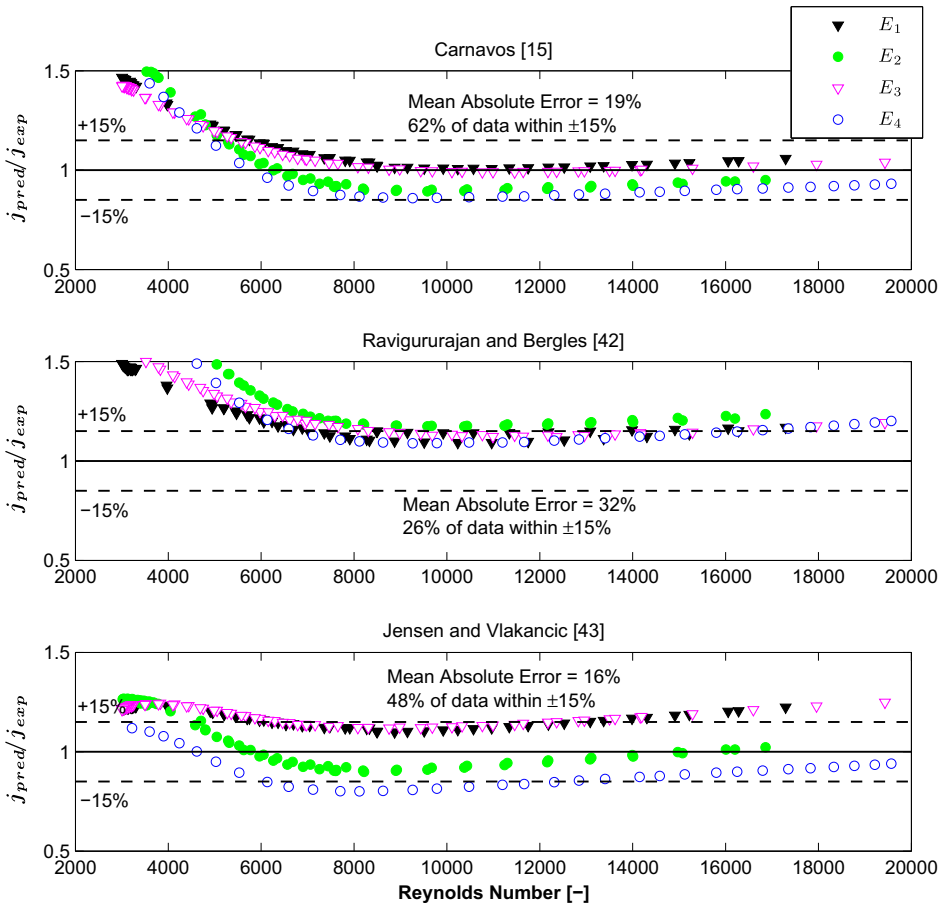

Fig. 7. Comparison of heat transfer data against the correlations of Carnavos [15], Ravigururajan and Bergles [42] and Jensen and Vlakancic [43].

$$Nu_{te} = \left[Nu_{Le}^{c1} + Nu_{Te_{38}}^{c1}\right]^{1/c1} \tag{16}$$

with $c1$ being a constant.

Since transition during the heat transfer process occurred between Reynolds numbers of 2000 and 3000, to extend the range of validity for this correlation, it was decided to use data for Reynolds numbers between 1900 and 4000. The best value for the constant to fit all the data was 7. Thus, the enhanced tube transition region heat transfer correlation is given as

$$Nu_{te} = \left[Nu_{Le}^{7} + Nu_{Te_{38}}^{7}\right]^{1/7} \tag{17}$$

for $1900 \leqslant Re \leqslant 4000$, $4.5 \leqslant Pr \leqslant 5.4$, $2.62 \times 10^5 \leqslant Gr \leqslant 4.45 \times 10^5$, $0.686 \leqslant \mu/\mu_w \leqslant 0.804$, $286 \leqslant L/D \leqslant 349$, $18^\circ \leqslant \beta \leqslant 27^\circ$, $0.176 \leqslant p_f/D \leqslant 0.387$ and $0.023 \leqslant e/D \leqslant 0.027$.

The performance of Eq. (17) is shown in Fig. 8, which is a combination of Eqs. 15 and 13. The correlation predicts 85% of the data to within 15%, having a mean absolute error of 9.4%.

5.2.4. Laminar flow: friction factor

From the diabatic smooth tube results in Olivier and Meyer [34], it was concluded that the increase in laminar friction factors was due to the buoyancy-induced secondary flow effects. It was shown that for enhanced tubes, however, additional friction is generated due to the helix angle. In Part I [29] it was shown that the adiabatic friction factor increase was only due to the fin height, and a correlation was developed. For the diabatic situation, however, additional terms would need to be added to incorporate the effect of mixed convection and secondary flows.

A proposed correlation would be to make use of the enhanced tube adiabatic correlation from Part I [29] and to add the necessary terms describing mixed convection. Included in this mixed convection term, however, the effects of the tube enhancement would need to be added. From the results, the only geometrical aspect of the enhanced tubes which had an effect on the friction factor was the helix angle. Thus, the form of the correlation would be

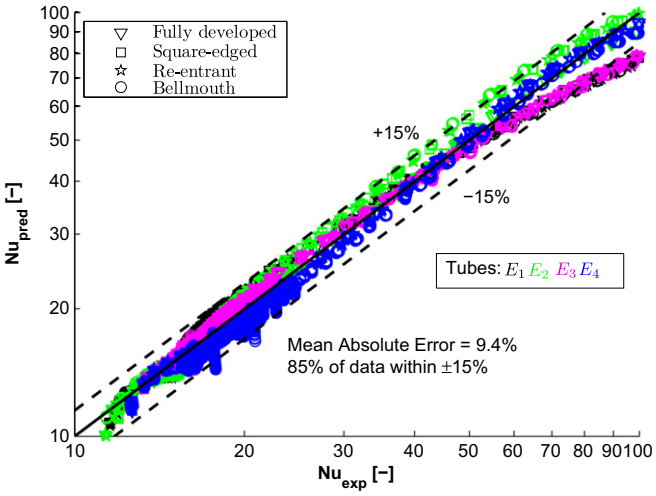

Fig. 8. Comparison of heat transfer data against the correlations given in Eqs. (13), (15) and (17).

$$f_{Le} = \frac{64}{Re}\left[1 + 88(e/D)^{2.2}Re^{0.2} + Gr^{c1}Pr^{c2}\left(\frac{D}{L}\right)^{c3}(\sin\beta)^{c4}\right] \quad (18)$$

Using the method of least squares, the constants, c_1, c_2, c_3 and c_4, were determined to be 0.49, −0.98, 0.71 and 1.04, respectively. These constants were obtained with a least-squares coefficient of 0.987. This correlation is valid for $1030 < Re < 2198$, $4.58 < Pr < 5.67$, $1.4 \times 10^5 < Gr < 2.5 \times 10^5$, $0.7 < \mu/\mu_w < 0.847$, $0.023 < e/D < 0.027$, $18^\circ < \beta < 27^\circ$ and $286 < L/D < 349$.

5.2.5. Turbulent flow: friction factor

The turbulent regime will be defined as Reynolds numbers between 2500 and 7000. Since the correlation of Jensen and Vlakancic [43] predicted the adiabatic friction factors very well [29], it was decided to make use of this correlation and add the necessary terms describing heat transfer. At the lower Reynolds numbers, one of the parameters which might still have an effect is the Grashof number. This is due to the secondary flow which might still be present in this region. A second parameter pertaining to fluid properties which has an influence on heat transfer is the Prandtl number. Further, to incorporate the effects between the wall and the bulk of the fluid, the viscosity ratio will also be included.

This correlation, in basic form, is given as

$$f_e/f_s = \left[(l_{csw}/D)^{c_1}(A_{cn}/A_c)^{c_2} - 0.0151\right.$$
$$\left./f_s\left[(l_{csw}/D)^{c_1}(A_{cn}/A_c)^{c_2} - 1\right]e^{-Re/c_3}\right]Pr^{c_4}Gr^{c_5}\left(\frac{\mu}{\mu_w}\right)^{c_6} \quad (19)$$

The definition of the characteristic length scale and nominal cross-sectional area will remain unchanged, and is given in Part I [29] of this paper. By the method of least squares, the constants were determined to be $c_1 = -2.2$, $c_2 = -46$, $c_3 = 5428$, $c_4 = 0.55$, $c_5 = -0.09$ and $c_6 = -1.2$. This correlation is valid for $2500 < Re < 6956$, $4.47 < Pr < 5.39$, $1.63 \times 10^5 < Gr < 4.45 \times 10^5$, $0.69 < \mu/\mu_w < 0.84$, $0.023 < e/D < 0.027$, $18^\circ < \beta < 27^\circ$ and $286 < L/D < 349$.

5.2.6. Transition flow: friction factor

From the discussion of the results, it was shown that the friction factors in the transition region were nearly independent of the Reynolds number. The fact that the slope in the transition region changes, though, would justify for a correlation to be developed. Since an adiabatic enhanced tube friction factor correlation was already developed [29], this correlation can be modified for diabatic flow. The Grashof and Prandtl numbers will be included to incorporate the mixed convection effects. Thus, the correlation will have the form

$$f_{te} = 4\left(\frac{16}{Re_{cr}}\right)^{c_1} exp\left(c_2\frac{Re}{Re_{cr}}\right)\left(\frac{\beta}{90}\right)^{c_3}\left(\frac{e^2}{p_f D}\right)^{c_4}$$
$$\times\left(\frac{p_f}{D}\right)^{c_5}\left(\frac{e}{D}\right)^{c_6}Pr^{c_7}Gr^{c_8}\left(\frac{\mu}{\mu_w}\right)^{c_9} \quad (20)$$

In this case, the critical Reynolds numbers for the different tubes were practically the same as for the fully developed flow data. Therefore, the correlation developed in Part I [29] for adiabatic fully developed flow was used, with critical Reynolds numbers varying between 1800 and 1900. Data was taken for Reynolds numbers greater than 2100 and less than 2600. The constants were determined by a least-squares optimisation method and are $c_1 = -0.131$, $c_2 = -0.111$, $c_3 = 2.363$, $c_4 = -0.313$, $c_5 = 0.766$, $c_6 = 0.786$, $c_7 = 0.081$, $c_8 = 0.028$ and $c_9 = -0.289$. This correlation is valid for $2105 < Re < 2596$, $4.47 < Pr < 5.33$, $2.8 \times 10^5 < Gr < 4.5 \times 10^5$, $0.69 < \mu/\mu_w < 0.8$, $0.023 < e/D < 0.027$, $18^\circ < \beta < 27^\circ$ and $286 < L/D < 349$.

Fig. 9 shows the performance of these three equations against the experimental data. The correlation predicts 97% of the data to within 20% with a mean absolute error of 5.5%. It is only the data of the square-edged and re-entrant for the 19.1 mm tubes (E_2 and E_3) that deviate from the laminar correlation.

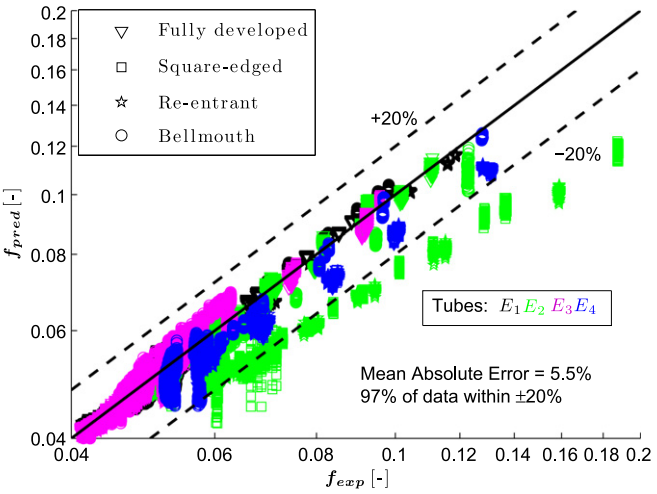

Fig. 9. Comparison of diabatic friction factor data against the correlations given in Eqs. (18)–(20).

6. Conclusion

Heat transfer and pressure drop data for enhanced tubes with different inlet geometries was investigated. The investigation covered the laminar, transitional and turbulent flow regimes.

Heat transfer results showed an overall increase when compared with the smooth tube values. This was brought about by the fins which break up the viscous sublayer. Further increases were attributed to the helix angle of the fins, spinning the fluid and enhancing the amount of mixing. Laminar results were slightly lower than the results of their smooth tube counterparts. This was attributed to the fins obstructing secondary flows, which are induced by buoyancy forces, reducing the amount of mixing. The fins have little or no effect on the spinning of the fluid due to the low velocity.

Transition, unlike adiabatic results, occurred at a Reynolds number of approximately 2000 and ended at approximately 3000. Transition occurred at these same Reynolds numbers, irrespective of the type of inlet used. This was also attributed to the secondary flows, which negate the influence of the inlet disturbance.

Friction factors showed similar trends as the heat transfer data. Turbulent friction factors were higher than those of their smooth tube counterpart, while laminar results showed the same increase obtained for the smooth tube data. The friction factor data also confirmed that transition was independent of the inlet profile used.

Correlations for each flow regime were developed to predict both the Nusselt numbers as well as diabatic friction factors. These correlations predicted the Nusselt number data with a mean absolute error of approximately 9.5%, predicting 85% of the data to within 15%. The friction factor correlations predicted the data with a mean absolute error of 5.5%, predicting 97% of the data to within 20%.

Acknowledgements

The following organisations are thanked for their support: the American Society of Heating, Refrigerating and Air-Conditioning Engineers (ASHRAE), which was the main sponsor of this project (RP-1280), the University of Pretoria, the Technology and Human Resources for Industry Programme (THRIP) – AL631, the Tertiary

Education Support Programme (TESP) from Eskom and the National Research Foundation and the SANERI/University of Stellenbosch Solar Hub.

References

[1] L. Tam, A.J. Ghajar, Effect of inlet geometry and heating on the fully developed friction factor in the transition region of a horizontal tube, Exp. Therm. Fluid Sci. 15 (1997) 52–64.

[2] O. Reynolds, On the experimental investigation of the circumstances which determine whether the motion of water shall be direct or sinuous, and the law of resistance in parallel channels, Philos. Tr. R. Soc. S. A–Math. Phys. Sci. 174 (1883) 935–982.

[3] E.R. Lindgren, Some aspects of the change between laminar and turbulent flow of liquids in cylindrical tubes, Arkiv för Fysik 7 (1953) 293–308.

[4] E.K. Kalinin, S.A. Yarkho, Flow pulsations and heat transfer in the transition region between the laminar and turbulent regimes in a tube, Int. Chem. Eng. 6 (1966) 571–574.

[5] A.J. Ede, The heat transfer coefficient for flow in a pipe, Int. J. Heat Mass Transfer 4 (1961) 105–110.

[6] H.R. Nagendra, Interaction of free and forced convection in horizontal tubes in the transition regime, J. Fluid Mech. 57 (1973) 269–288.

[7] A.J. Ghajar, K.F. Madon, Pressure drop measurements in the transition region for a circular tube with three different inlet configurations, Exp. Therm. Fluid Sci. 5 (1992) 129–135.

[8] A.M.O. Smith, Remarks on transition in a round tube, J. Fluid Mech. 7 (1960) 565–576.

[9] A.J. Ghajar, L. Tam, Heat transfer measurements and correlations in the transition region for a circular tube with three different inlet configurations, Exp. Therm. Fluid Sci. 8 (1994) 79–90.

[10] A.J. Ghajar, L.M. Tam, Laminar-transition-turbulent forced and mixed convective heat transfer correlations for pipe flows with different inlet configurations, HTD, Fundam. Forced Convective Heat Transfer, ASME 181 (1991) 15–23.

[11] Y. Mori, K. Futagami, S. Tokuda, M. Nakamura, Forced convective heat transfer in uniformly heated horizontal tubes, Int. J. Heat Mass Transfer 9 (1966) 453–463.

[12] W. Nunner, Heat transfer and pressure drop in rough tubes, VDI-Forschungsheft 455-B (1956) 5–39.

[13] N.T. Obot, E.B. Esen, T.J. Rabas, The role of transition in determining friction and heat transfer in smooth and rough passages, Int. J. Heat Mass Transfer 33 (1990) 2133–2143.

[14] R. Koch, Pressure loss and heat transfer for turbulent flow, Atomic Ener. Commission Translation Ser. 3875 (1960) 1–135.

[15] T.C. Carnavos, Heat transfer performance of internally finned tubes in turbulent flow, Heat Transfer Eng. 1 (1980) 32–37.

[16] J.G. Withers, Tube-side heat transfer and pressure drop for tubes having helical internal ridging with turbulent/transitional flow of single-phase fluid. Part 1. Single-helix ridging, Heat Transfer Eng. 2 (1980) 48–58.

[17] J.G. Withers, Tube-side heat transfer and pressure drop for tubes having helical internal ridging with turbulent/transitional flow of single-phase fluid. Part 2. Multiple-helix ridging, Heat Transfer Eng. 2 (1980) 43–50.

[18] C.B. Chiou, C.C. Wang, D.C. Lu, Single-phase heat transfer and pressure drop characteristics of microfin tubes, ASHRAE Trans.: Symposia 11 (1995) 1041–1048.

[19] C.C. Wang, C.B. Chiou, D.C. Lu, Single-phase heat transfer and flow friction correlations for microfin tubes, Int. J. Heat Fluid Flow 17 (1996) 500–508.

[20] L.J. Brognaux, R.L. Webb, L.M. Chamra, B.Y. Chung, Single-phase heat transfer in micro-fin tubes, Int. J. Heat Mass Transfer 40 (1997) 4345–4357.

[21] S. Eiamsa-ard, P. Promvonge, Experimental investigation of heat transfer and friction characteristics in a circular tube fitted with V-nozzle turbulators, Int. Commun. Heat Mass Transfer 33 (2006) 591–600.

[22] L.D. Tijing, B.C. Pak, B.J. Baek, D.H. Lee, A study on heat transfer enhancement using straight and twisted internal fin inserts, Int. Commun. Heat Mass Transfer 33 (2006) 719–726.

[23] W.J. Marner, A.E. Bergles, Augmentation of highly viscous laminar heat transfer inside tubes with constant wall temperature, Exp. Therm. Fluid Sci. 2 (1989) 252–267.

[24] R.M. Manglik, A.E. Bergles, Heat transfer and pressure drop correlations for twisted-tape inserts in isothermal tubes: Part 1 - laminar flows, J. Heat Transfer 115 (1993) 881–889.

[25] S.F. Al-Fahed, L.M. Chamra, W. Chakroun, Pressure drop and heat transfer comparison for both microfin tube and twisted-tape inserts in laminar flow, Exp. Therm. Fluid Sci. 18 (1999) 323–333.

[26] S.K. Saha, A. Dutta, S.K. Dhal, Friction and heat transfer characteristics of laminar swirl flow through a circular tube fitted with regularly spaced twisted-tape elements, Int. J. Heat Mass Transfer 44 (2001) 4211–4223.

[27] A. García, P.G. Vicente, A. Viedma, Experimental study of heat transfer enhancement with wire coil inserts in laminar-transition-turbulent regimes at different Prandtl numbers, Int. J. Heat Mass Transfer 48 (2005) 4640–4651.

[28] A. García, J.P. Solana, P.G. Vicente, A. Viedma, Enhancement of laminar and transitional flow heat transfer in tubes by means of wire coil inserts, Int. J. Heat Mass Transfer 50 (2007) 3176–3189.

[29] J.P. Meyer, J.A. Olivier, Transitional flow inside enhanced tubes for fully developed and developing flow with different types of inlet disturbances: Part I – Adiabatic pressure drops, Int. J. Heat Mass Transfer 54 (2011) 1587–1597.

[30] IAPWS, Uncertainties in Enthalpy for the IAPWS Formulation 1995 for the Thermodynamic Properties of Ordinary Water Substance for General and Scientific Use (IAPWS-95) and the IAPWS Industrial Formulation 1997 for the Thermodynamic Properties of Water and Steam (IAPWS),Technical Report, International Association for the Properties of Water and Steam, 2003.

[31] S.I. Abu-Eishah, Correlations for the thermal conductivity of metals as a function of temperature, Int. J. Thermophys. 22 (2001) 1855–1868.

[32] A. Lambrechts, Heat Transfer Performance during In-tube Condensation in Horizontal Smooth, Micro-fin and Herringbone Tubes, M. Eng. dissertation, University of Johannesburg, 2003.

[33] W. Wagner, A. Pruß, The IAPWS formulation 1995 for the thermodynamic properties of ordinary water substance for general and scientific use, J. Phys. Chem. Ref. Data 31 (2002) 387–535.

[34] J.A. Olivier, J.P. Meyer, Single-phase heat transfer and pressure drop by means of the cooling of water inside smooth tubes for transitional flow with different inlet geometries (RP-1280), HVAC&R Res. 16 (2010) 471–496.

[35] E.N. Sieder, G.E. Tate, Heat transfer and pressure drop in liquids in tubes, Indus. Eng. Chem. 28 (1936) 1429–1435.

[36] D.R. Oliver, The effect of natural convection on viscous-flow heat transfer in horizontal tubes, Chem. Eng. Sci. 17 (1962) 335–350.

[37] B. Shome, M.K. Jensen, Mixed convection laminar flow and heat transfer of liquids in isothermal horizontal circular ducts, Int. J. Heat Mass Transfer 38 (1995) 1945–1956.

[38] B. Metais, E.R.G. Eckert, Forced, mixed and free convection regimes, Trans. ASME J. Heat Transfer 10 (1964) 295–296.

[39] W.J. Marner, A.E. Bergles, J.M. Chenoweth, On the presentation of performance data for enhanced tubes used in shell-and-tube heat exchangers, J. Heat Transfer 105 (1983) 358–365.

[40] R.K. Shah, D.P. Seculić, Fundamentals of Heat Exchanger Design, John Wiley and Sons Inc, New Jersey, 2003.

[41] P.G. Vicente, A. García, A. Viedma, Experimental study of mixed convection and pressure drop in helically dimpled tubes for laminar and transition flow, Int. J. Heat Mass Transfer 45 (2002) 5091–5105.

[42] T.S. Ravigururajan, A.E. Bergles, Development and verification of general correlations for pressure drop and heat transfer in single-phase turbulent flow in enhanced tubes, Exp. Therm. Fluid Sci. 13 (1996) 55–70.

[43] M.K. Jensen, A. Vlakancic, Experimental investigation of turbulent heat transfer and fluid flow in internally finned tubes, Int. J. Heat Mass Transfer 42 (1999) 1343–1351.

[44] J.A. Olivier, Single-Phase Heat Transfer and Pressure Drop of Water Cooled at a Constant Wall Temperature Inside Horizontal Circular Smooth and Enhanced Tubes with Different Inlet Configurations in the Transitional Flow Regime, Ph.D. thesis, Department of Mechanical and Aeronautical Engineering, University of Pretoria, 2009.

[45] S.W. Churchill, R. Usagi, A general expression for the correlation of rates of transfer and other phenomena, J. American Institut. Chem. Eng. 18 (1972) 1121–1128.